International Journal of Heat and Mass Transfer 82 (2015) 267–272

Contents lists available at ScienceDirect

International Journal of Heat and Mass Transfer

journal homepage: www.elsevier.com/locate/ijhmt

Broadband radiative energy absorption using a silicon nanowire forest with silver nanoclusters for thermal energy conversion

Beom Seok Kim [a], Sikandar H. Tamboli [a], Jae Baek Han [b], Taehwan Kim [a], Hyung Hee Cho [a,*]

[a] Department of Mechanical Engineering, Yonsei University, 50 Yonsei-ro, Seodaemun-gu, Seoul 120-749, Republic of Korea
[b] Republic of Korea Air Force, 18th Fighter Wings PO box 334, Gangneung, Gangwondo, Republic of Korea

ARTICLE INFO

Article history:
Received 10 May 2014
Received in revised form 7 November 2014
Accepted 10 November 2014
Available online 6 December 2014

Keywords:
Energy conversion
Heat transfer
Radiative absorbance
Surface modification
Silicon nanowires
Nanocluster

ABSTRACT

Heat transfer based on radiative energy absorption and thermal dissipation is important in the design of energy conversion and transfer systems. We studied in the design of radiative energy absorber for efficient energy harvesting and transfer using a nanoscale interface modification technology. We presented that silver nanoclusters assisted silicon nanowires (SiNWs) forest could be feasible for radiative energy absorption in a broadband spectral region. A drastic increase of radiative energy absorption could be obtained in the near infrared wavelength region with accompanying quasi-perfect absorption (higher than 95%) of ultra-violet and visible range of the irradiation spectrum. All of surface manipulations were based on top-down metal-assisted chemical etching feasible under room-temperature conditions to synthesize SiNWs with silver nanoclusters. The spectral absorbance characteristics were elucidated for characteristic lengths of SiNWs, clustering of silver nanoparticles, orientation of the substrate, and single as well as double-sided silver nanoclusters orientations dominate in spectral absorbance characteristics. The results were also presented for guaranteeing efficient solar-thermal converting components with 92.4% solar absorption performance under AM1.5D condition. Surface modification and optimization will be helpful to improve the performances of solar energy conversion systems and various heat transfer systems.

1. Introduction

Solar-thermal energy conversion is one of the most intriguing applications of renewable and sustainable energy supply. The solar-thermal conversion efficiency definitely depends on the radiative solar absorption at a solid interface and subsequent conductive heat transfer through the solid media [1–7]. Especially for efficient solar absorption, modern nanotechnology has suggested a feasible way to drastically increase radiative solar absorption performances [8,9]. Design changes to the interface surface have been attempted by structural modification with respect to 3-dimensional structure formation including meta-materials with novel architectures [10–12] as well as surface roughening [13–17], modulation of the refractive index [18], and reflection control [19]. Through the recent research, it has been confirmed that light scattering and trapping within the manipulated interfacial solid media increase the radiative absorbance, and it could be possible by manipulating exquisite architectures with the characteristic lengths below the wavelength of irradiation.

To meet the requirements for efficient photo-thermal conversion systems, we have to select an appropriate material at first for the solid substrate, which have a high thermal conductivity and feasibility to realize the interfacial structures. Considering the backgrounds and effectiveness, silicon (Si) can be one of the promising elements most responsible for the next generation of sustainable energy-harvesting technology and to power generation due to its intrinsic band-gap property, thermal conductivity, manufacturing feasibility, and abundance on the earth. However, there is room for improvement in Si-based substrates [20–23]. It has almost transparent characteristics under infrared (IR) irradiation due to its intrinsic band-gap properties. Even though most solar-irradiating energy is concentrated in the ultra-violet (UV) and visible (VIS) wavelength spectra, the resulting limitation in the performance of thermal-conversion systems as well as solar-absorbing systems could be resolved by extending the high-absorbance domain to complementary parts of the irradiation spectrum in the IR region [24].

In this study, we present that highly efficient radiative energy absorption in the near-IR (NIR) region can be realized with accompanying quasi-perfect absorbance in the UV–VIS spectrum. The structure- and material-induced light-trapping method, which is

* Corresponding author. Tel.: +82 2 2123 2828; fax: +82 2 2123 8247.
E-mail address: hhcho@yonsei.ac.kr (H.H. Cho).

http://dx.doi.org/10.1016/j.ijheatmasstransfer.2014.11.043
0017-9310/

attributable to a forest of vertically aligned silicon nanowire arrays (SiNWs) in the form of 'black silicon' and silver nanoclusters (Ag-NCs) as a 'plasmonic light confiner', is discussed. We also highlight the role of Ag-NCs as a plasmonic light confiner; the presence of Ag-NCs at the base of the SiNWs. The radiative absorption characteristics are elucidated with respect to the characteristic dimensions of SiNWs, clustering of Ag, and structure of the absorbing system, in terms of the orientation of the substrate and double-side effects. A feasible and simple top-down method that is appropriate for room temperature processing is proposed, and it could be used for reliable mass production of large-areal synthesis. The characteristics and demonstrated strategies on efficient absorption of radiative energy can also widen its application fields towards heat transfer and cooling systems such as heat sinks, thermal spreaders, and heat exchangers [25,26].

2. Materials and methods

2.1. Fabrication method for top-down SiNWs w/Ag clusters

Vertically aligned SiNWs with and without Ag-NCs are synthesized by a metal-assisted chemical etching method (MaCE) [27–29]. A 525-micron-thick silicon substrate is immersed in a solution of 4.8 M HF and 0.005 M $AgNO_3$ to introduce the metallic ions of Ag^+ onto the substrate surface by galvanic displacement [30]. After the reduction of Ag for 1 min, the substrate is etched with an etching solution that is a mixture of 4.8 M HF and 0.1 M H_2O_2. In the solution, the oxidized area of Si just below the reduced silver particles is etched away by hydrofluoric acid, and those partial areas henceforth becomes deeper, forming nanoholes on the substrate. The residual area that does not undergo the etching process consequently forms vertically aligned SiNWs. The height of SiNWs, as a characteristic length of the structure, is principally controlled by changing the etching time of the Si substrates in the solution of HF and H_2O_2. However, the reduced silver particles remain at the bottom of the nanoholes as nanoclusters. These can be dissolved using nitric acid solution. For comparative demonstrations of the effect of Ag-NCs, additional samples with an intentional silver thin layer (40 nm) are fabricated by conformal Ag deposition using an E-beam evaporator on the synthesized SiNWs without Ag-NCs. The SEM images and apparent length of SiNWs (l), that is, the ratio of the total etched depth on both sides of substrate to the initial thickness of the substrate (525 μm), are presented in Table 1 and Fig. 1, respectively. The whole wet-bench procedure is conducted under room temperature and atmospheric pressure conditions.

2.2. Surface characterizations

The surface morphology was characterized by field emission scanning electron microscopy (FE-SEM, JSM-6700F, JEOL), and we confirmed the average height of the SiNWs with image processing. Composition analysis on the nanoclusters and conformally deposited Ag was conducted in the backscattered electron imaging mode, and images presenting the nanoclusters on the bottom of nanoholes between SiNWs were compared with the conformally Ag-deposited samples. The SEM images and apparent length of SiNWs (l) are presented in Fig. 1 and Table 1 in the manuscript, respectively.

2.3. Measurement of spectral absorbance

The spectral absorbance of the prepared samples was evaluated by measuring the spectral reflectance and transmittance. The total hemispherical reflectance and transmittance were measured using a spectrophotometer (Cary5000, Agilent) with an integrating sphere. The spectral range of irradiation was in a range of UV to NIR from 200 to 2200 nm, where effective energy transformation could be feasible with the high spectral irradiance of solar irradiation. The spectral absorbance was consequently evaluated based on the formula $\alpha(\lambda) = 1 - (r(\lambda) + T(\lambda))$, where $\alpha(\lambda)$, $r(\lambda)$, $T(\lambda)$ and λ represent spectral absorbance, spectral reflectance, spectral transmittance, and wavelength of irradiation, respectively.

3. Results and discussion

3.1. Structural light scattering characteristics and SiNWs dimension

Structural light scattering characteristics are principal factors for light absorbance. Fig. 2 presents that absorbance is greatly dependent on the effects of the characteristic dimension of interfacial structures, that is, the height of SiNWs. For efficient light absorption, the characteristic physical length of the superficial structures should catalyze light scattering to increase the optical path length. Vertically aligned SiNWs can play a role as an anti-transmission and anti-reflection layer, causing light scattering that disturbs the straight incidence of irradiating light. This makes the dense forest of SiNWs favorable for enhancing light-trapping performance [14,20,31]. The morphological characteristics of SiNWs are effective in realizing ultrahigh surface area, subwavelength structure, and compensative porosity gradient changing refractive index with depth, which are essential for an effective light-absorbing surface [12,13,16,26]. Based on those merits, we demonstrate that SiNWs in the form of black silicon have near-perfect light-absorption performance, especially in the region of UV to VIS spectra. All of the samples, from 2 to 22 microns in height, have high absorbance, α, namely over 90% from 200- to 1000-nm-wavelength incident light. However, silicon is an inherently IR-transparent material with low light-absorbing characteristics, thus the spectral absorbance in NIR from 1100 to 2200 nm is <40%. As we increased the characteristic length, h, of SiNWs, clear enhancement of absorption was apparent, especially in the NIR region. From the inset of Fig. 2, we can confirm that the increase in the characteristic length induced a definite improvement in absorption in the NIR region. Herein, the normalized efficiency, η, the ratio of the average

Table 1
Fabricated samples of SiNWs accompanying Ag treatments. The column marked 'Sides' shows the surface where SiNWs are synthesized. The apparent length of SiNWs, l, (the ratio of the total etched depth on both sides of the substrate to the initial thickness of the substrate) depends on the etching time during the synthesis of SiNWs and the sides. The initial thickness of the substrate is 525 μm.

Case	SiNWs			Ag	Case	SiNWs			Ag
	Sides	h (μm)	l			Sides	h (μm)	l	
Pl	–	–	–	–	*SN5*	Double	10.1	0.039	–
SN1	Single	2.4	0.005	–	*SN6*	Single	10.1	0.019	Ag-NCs
SN2	Single	7.1	0.014	–	*SN7*	Double	10.1	0.039	Ag-NCs
SN3	Single	10.1	0.019	–	*SN8*	Double	10.1	0.039	40-nm deposition, front
SN4	Single	21.1	0.040	–	*SN9*	Double	10.1	0.039	40-nm deposition, rear

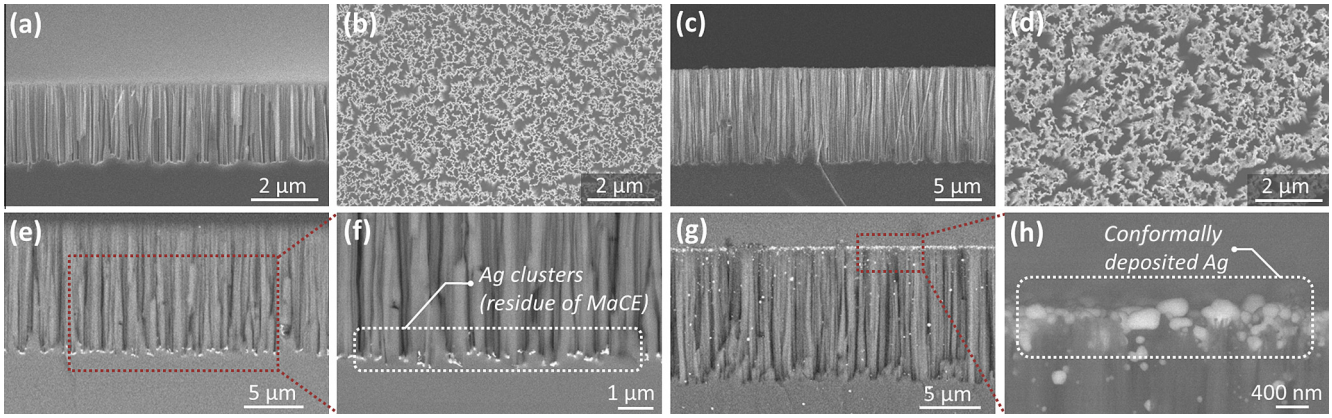

Fig. 1. FE-SEM images for synthesized SiNWs. (a, b) Cross-sectional and top view of *SN1* etched for 5 min without Ag clusters. (c, d) Cross-sectional and top view of *SN3* etched for 30 min without Ag clusters. (e, f) SiNWs (*SN7*) with Ag clusters which are residues of the MaCE. (g, h) SiNWs (*SN8*) with deposited Ag layer, which are formed by E-beam evaporation. Herein, (e, f, g) and (h) are taken in composition mode.

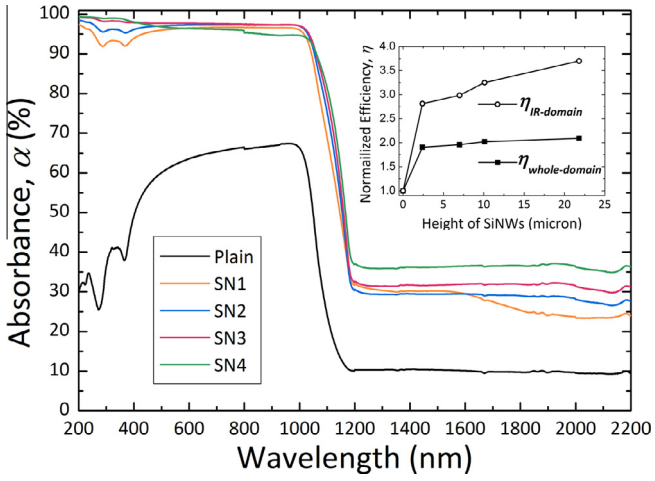

Fig. 2. Spectral absorbance curves according to characteristic dimensions of the height of SiNWs from the UV to the NIR region. The inset presents the normalized efficiency, $\bar{\alpha}/\bar{\alpha}_{Pl}$, i.e., the relative absorbance compared with the plain Si substrate at the wavelength of the corresponding spectral region.

of spectral absorbance to that of the plain silicon substrate (*Pl*), is defined as follows:

$$\eta = \bar{\alpha}/\bar{\alpha}_{Pl} \tag{1}$$

where the subscripts indicate the corresponding wavelength region (i.e., either total or NIR region). In the UV and visible spectrum range with short wavelength, remarkably high absorbance accompanying low reflectance can be attributed to the ultrahigh surface area and subwavelength structured surface created by the SiNWs [14]. On the other hand, the longer characteristic length of SiNWs, which generate a kind of texturing or grating structure such as the forest-like SiNWs on the substrate, can be favorable to enhance light trapping. The characteristic length sufficient for the constructive interference or confinement of diffracted or scattered long-wavelength light inside the light-absorbing layer should be guaranteed [32]. Therefore, vertically aligned and long SiNWs with a micron-scale characteristic length are appropriate for IR scattering to improve the absorbance of incident light with a long-wavelength.

3.1. Effects of double-sided light scattering and plasmonic light confinement

Double-sided SiNWs (*SN5*) enhance absorbance in NIR by 34.8% and 25.9% compared with single-sided SiNWs of *SN3* and *SN4*,

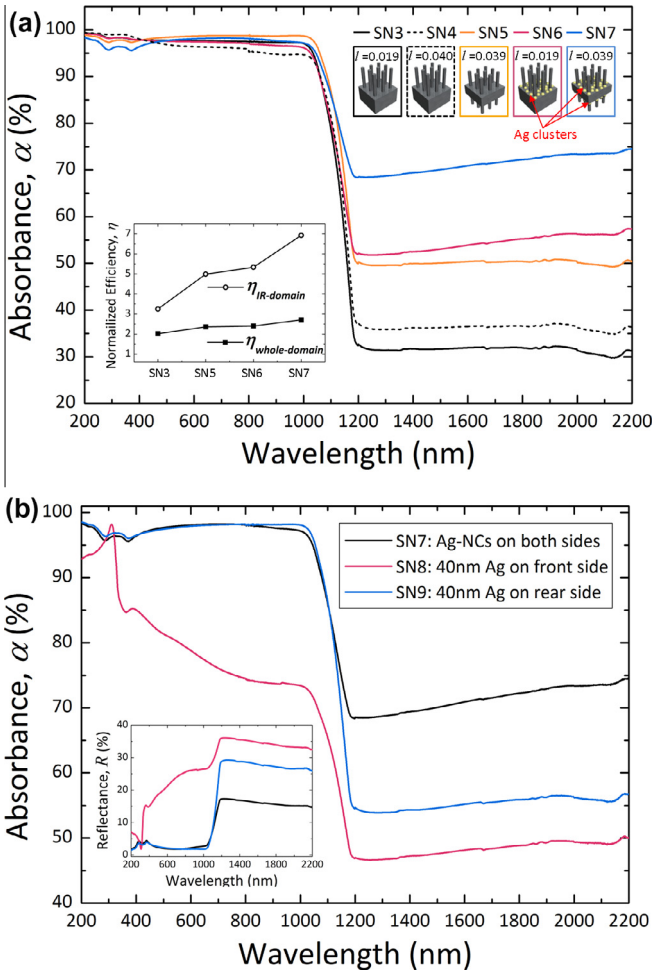

Fig. 3. Spectral absorbance curves. (a) Effects of double-sided SiNWs and Ag nanoclusters. The inset of (a) shows the evaluated normalized efficiency for each sample at the corresponding spectral region wavelength. (b) Comparison of nanoclustered Ag with conformally deposited Ag and the orientation effects of the latter sample relative to the reflecting layer. The inset of (b) presents the spectral reflectance from *SN7*, *SN8*, and *SN9*.

respectively, as shown in Fig. 3(a). This results from the decrease in both reflection and transmission of irradiative light due to the reinforcing of light scattering with depth and backside scattering.

From the comparison between *SN4* and *SN5*, we can confirm that double-sided is more effective than single-sided scattering. *SN5*, whose apparent length, l (presented in Table 1), is quasi-equivalent to *SN3* on both sides, has much higher absorbance characteristic in the NIR region. In the case of single-sided SiNWs, most of the light scattering occurs on the front-facing side of the substrate due to the rough SiNWs. On the other hand, double-sided SiNWs are effective in confining incident light in the solid media by increasing the effective sites of wave impingements causing secondary scattering on both sides. The disordered SiNWs-forest at the rear of the substrate can lead to additional disturbance of the already-attenuated incident light that passed through the front scattering forest and the substrate, as well as partial scattering backward at the rear of the substrate. Accordingly, the increased scattering sites empower the constructive interference of waves in the solid media. Therefore, double-sided scattering can be more effective to improve NIR absorption compared with single-sided scattering under the quasi-equivalent interfacial surface roughness of l.

From Fig. 3(a), we can explain the role of Ag-NCs on the bottom of nanoholes between SiNWs, as a plasmonic light confiner, have great effects on NIR absorption enhancement. Single-sided SiNWs with Ag-NCs (*SN6*) have higher absorbance than did double-sided SiNWs without Ag-NCs, and the disparity becomes wider in the NIR region. The sample of *SN7*, which has double-sided SiNWs with Ag-NCs, has the highest average absorbance of 83.2% and 71.8% in the overall spectral region and NIR region, respectively. This enhancement can be explained by the effects of the metallic nanoclusters, which result in light confinement via plasmonic effect [33–35]. Nanoscale noble metal particles, such as Au or Ag, lead to a collective oscillation of conduction electrons against incident electromagnetic radiation and result in surface plasmonic resonance. The electric field of the incoming radiation induces the dipole formation in the metallic nanoparticles, and it results in the counteracting restoring force that tries to compensate it [36]. According to the intrinsic Ag particle size and particle-interaction effects, those metallic particles can be used to improve NIR-absorbing performances. Within a SiNWs-forest the densely distributed Ag-NCs, whose diameters are from tens of to hundreds of nanometers and interparticle distance is close with a high volume fraction of the particles, can promote red-shift and broadening of the plasmon band with high absorption in NIR due to reinforced dipole–dipole interactions [36,37]. As a result, Ag-NCs at the base SiNWs on the substrate induce light confinement based on the surface plasmonic resonance. The subsequent scattering in the forests of vertically standing SiNWs can create a synergy effect for improved light trapping appropriate to NIR on the solid interface.

The orientation of the metallic reflector is another essential design factor for efficient light trapping [32,38,39]. The curves for *SN8* and *SN9* in Fig. 3(b) show the results for spectral absorbance variation according to the forward- and backward-oriented metallic reflector. Even though *SN8* has the metallic reflection layer with extremely rough SiNWs on the substrate, absorbance is low, with $\bar{\alpha}_{UV-VIS}$ of 80.8% even in the region of wavelengths of 200–1000 nm. Otherwise, *SN9* which has a backside reflection layer, has quasi-perfect (97.7%) and outstanding (>55%) light-absorption performance in the UV–VIS and NIR regions, respectively. For a preferable method for absorbance enhancement, the reflector should play a role in light trapping by lengthening the optical path-length of incident light. If the reflector faces frontward against incidence, most of reflection happens on the front-facing interface. However, the optical path length could be increased if the reflector is located at the rear of the substrate. Even though the thickness of the substrate is about hundreds of microns, reflected light at the rear can not only form constructive interference through the substrate but also induce backward scattering in the front SiNWs forest once again. This difference in the orientation of a metallic reflector results in a clear improvement in the absorbance for the backside reflector in the UV–VIS as well as NIR region.

The effects of Ag-NCs can also be demonstrated by comparing them with a metallic uniform layer made by conformal deposition of Ag shown in Fig. 1(g) and (h). Fig. 3(b) shows that the conformally deposited Ag layer of *SN8* and *SN9* results in low light-absorption compared with the metallic Ag-NCs of *SN7*. As shown in the inset of Fig. 3(b), the conformally deposited Ag layer on top of SiNWs is available to increase reflectivity in the range of UV to NIR as a forward-oriented reflection layer. A backward-oriented reflection layer (*SN9*), however, has somewhat similar absorbing characteristics to SiNWs with Ag-NCs. Even though the spectral absorbance is slightly less than that of SiNWs with Ag-NCs in the NIR region, it would be effective for increasing the optical path length with reduced light loss due to reflectance. Based on the results, we demonstrate that nanoclusters are very effective as a light confiner for absorbance improvement, especially for the NIR, and the orientation of a metallic reflector layer should be a critical design factor. The conformally deposited Ag reflector could be an alternative idea to match the synthesis of nanoscale clusters with SiNWs based on the MaCE method.

3.2. Absorption improvement by SiNWs with Ag-NCs

Fig. 4 illustrates the structure of SiNWs with Ag-NCs and depicts light confinement for the absorbance improvement. The resulting ultrahigh absorbance can be explained by the combined effects of light scattering by extremely rough SiNWs and plasmonic light confinement by Ag-NCs. The respective roles of the structural and material characteristics lead to effective light confinement in the solid medium of Si at wavelengths from UV to long-wavelength NIR. At short wavelengths, structures with small characteristic length are effective for absorbance enhancement. The majority of previous approaches has been based on roughening the surface morphology by creating submicron structures, so that the incoupling of short-wavelength light can be improved. Larger structures have been favored for long-wavelength light due to the wavelength-matched light-trapping mechanism of the constructive interference of the diffracted wave, especially on an interfacial surface and through a solid medium [32]. For silicon, whose IR absorbance is intrinsically low, light trapping by maximizing diffraction through the medium is essential. Especially for short wavelengths, most of the absorption occurs near the interface. However, diffraction in the media and scattering by backside reflector are keys to improving absorption performance for longer wavelengths [32]. Based on this physics, maximizing interference between the incident wave and diffraction in media can be improved by a forest of double-sided SiNWs that extend the optical path length. Light confinement can be guaranteed for NIR absorbance by maximizing the optical path length that accompanies the scattering and diffraction through the media via long SiNWs and plasmonic confinement via Ag-NCs [35,40,41].

Long-wavelength light absorption can consequently improve solar energy absorption. Fig. 5 presents the spectral performance of solar energy absorption under AM1.5D irradiation. Herein, the efficiency of energy absorption, θ is defined to quantify the total efficiency of solar absorption as follows [42]:

$$\theta_i = \frac{\int I_{AM1.5D}(\lambda)\cdot\alpha_i(\lambda)d\lambda}{\int I_{AM1.5D}(\lambda)d\lambda} \quad (2)$$

where $I_{AM1.5D}(\lambda)$ and $\alpha_i(\lambda)$ represent spectral irradiance of AM1.5D and spectral absorbance, respectively. Here, the subscript i represents the corresponding domain of wavelength. It is concluded that SiNWs with Ag-NCs have excellent efficiency of 92.4% and 71.1% in

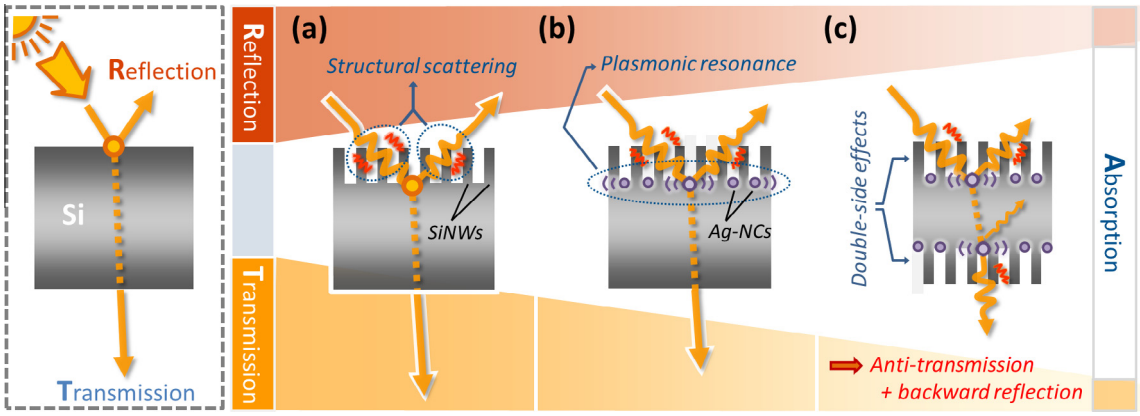

Fig. 4. Schematics on structural light scattering and plasmonic light confinement in solid media for the increase in absorbance by SiNWs with Ag-NCs. (a) Structural light scattering via densely distributed single-side SiNWs. (b) Plasmonic lateral light confinement combined with the SiNWs for light scattering. (c) Structural and plasmonic effects accompanying secondary light absorption by backside reflecting and scattering via double-sided SiNWs with Ag-NCs.

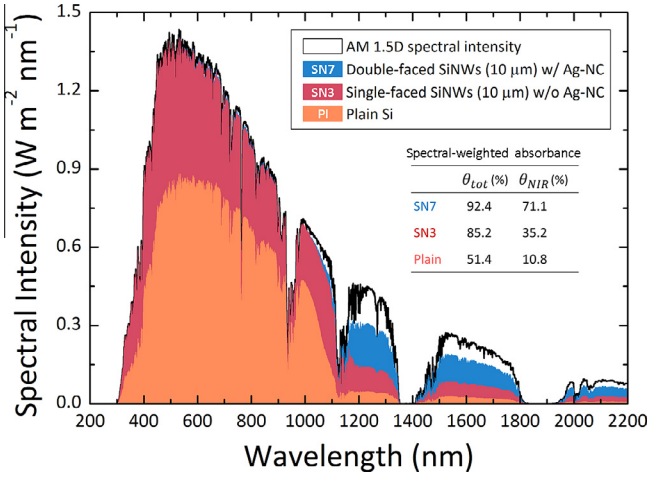

Fig. 5. Spectral energy absorption under the AM1.5D reference spectrum with the quantified spectral-weighted absorbance for the samples of *Pl*, *SN3*, and *SN7*.

the overall wavelength domain from 200 to 2200 nm and the NIR domain from 1100 to 2200 nm, respectively. This is outstanding because silicon as a substrate has been treated as an inefficient material, especially for irradiative energy absorbance in the IR region. In the NIR region, the efficiency is improved by more than 558% compared with that of a plain silicon substrate.

4. Conclusion

We demonstrate that highly efficient solar energy absorption can be realized with accompanying quasi-perfect absorbance in the UV–VIS spectrum. A structure- and material-induced light-trapping system consists of a forest of SiNWs as black silicon and Ag-NCs as a plasmonic light confiner, and suggests highest 92.4% solar absorption under AM1.5D condition. The spectral absorbance characteristics are elucidated with respect to the characteristic dimensions of SiNWs, clustering of Ag, and structure of the absorbing system including the orientation of the substrate and the double-sided effects. Ag-NCs are effective in guaranteeing NIR absorption performance. The feasible and simple MaCE method appropriate for room temperature processing could be plausible for silver nanoclusters assisted SiNWs forest mass production as well as large area synthesis. The demonstrated characteristics on efficient absorption of radiative energy can also widen its application fields towards various engineering fields. Surface modification and optimization would present a breakthrough not only in solar-energy conversion systems but also in cooling and heat transfer systems.

Conflict of interest

The authors declare no competing financial interest.

Acknowledgments

This work was supported by a National Research Foundation of Korea (NRF) Grant funded by the Korea government (MEST) (No. 2011-0017673) and by the Low Observable Technology Research Center program of Defense Acquisition Program Administration and Agency for Defense Development. The author B.S. Kim is grateful for a Seoul Science Fellowship provided by the Seoul Metropolitan Government.

References

[1] A. Sayigh, Renewable energy – the way forward, Appl. Energy 64 (1999) 15–30.
[2] C.G. Granqvist, Solar energy materials, Adv. Mater. 15 (2003) 1789–1803.
[3] S.A. Kalogirou, Solar thermal collectors and applications, Prog. Energy Combust. Sci. 30 (2004) 231–295.
[4] D. Mills, Advances in solar thermal electricity technology, Sol. Energy 76 (2004) 19–31.
[5] T. Mateus, A.C. Oliveira, Energy and economic analysis of an integrated solar absorption cooling and heating system in different building types and climates, Appl. Energy 86 (2009) 949–957.
[6] A. Hobbi, K. Siddiqui, Experimental study on the effect of heat transfer enhancement devices in flat-plate solar collectors, Int. J. Heat Mass Transfer 52 (2009) 4435–4448.
[7] R. Bayón, E. Rojas, Simulation of thermocline storage for solar thermal power plants: from dimensionless results to prototypes and real-size tanks, Int. J. Heat Mass Transfer 60 (2013) 713–721.
[8] H. Chen, L. Shao, T. Ming, Z. Sun, C. Zhao, B. Yang, J. Wang, Understanding the photothermal conversion efficiency of gold nanocrystals, Small 6 (2010) 2272–2280.
[9] T.T. Chow, A review on photovoltaic/thermal hybrid solar technology, Appl. Energy 87 (2010) 365–379.
[10] C. Hägglund, G. Zeltzer, R. Ruiz, I. Thomann, H.B.R. Lee, M.L. Brongersma, S.F. Bent, Self-assembly based plasmonic arrays tuned by atomic layer deposition for extreme visible light absorption, Nano Lett. 13 (2013) 3352–3357.
[11] C. Wu, B. Neuner III, J. John, A. Milder, B. Zollars, S. Savoy, G. Shvets, Metamaterial-based integrated plasmonic absorber/emitter for solar thermo-photovoltaic systems, J. Opt. 14 (2012) 024005.
[12] J. Hao, J. Wang, X. Liu, W.J. Padilla, L. Zhou, M. Qiu, High performance optical absorber based on a plasmonic metamaterial, Appl. Phys. Lett. 96 (2010) 251104.
[13] Y. Kanamori, M. Sasaki, K. Hane, Broadband antireflection gratings fabricated upon silicon substrates, Opt. Lett. 24 (1999) 1422–1424.

[14] K.Q. Peng, X. Wang, S.T. Lee, Silicon nanowire array photoelectrochemical solar cells, Appl. Phys. Lett. 92 (2008) 163103.
[15] H.M. Branz, V.E. Yost, S. Ward, K.M. Jones, B. To, P. Stradins, Nanostructured black silicon and the optical reflectance of graded-density surfaces, Appl. Phys. Lett. 94 (2009) 231121.
[16] E.A. Santori, J.R. Maiolo III, M.J. Bierman, N.C. Strandwitz, M.D. Kelzenberg, B.S. Brunschwig, H.A. Atwater, N.S. Lewis, Photoanodic behavior of vapor–liquid–solid-grown, lightly doped, crystalline Si microwire arrays, Energy Environ. Sci. 5 (2012) 6867–6871.
[17] W.C. Wang, C.W. Lin, H.J. Chen, C.W. Chang, J.J. Huang, M.J. Yang, B. Tjahjono, W.C. Hsu, M.J. Chen, Surface passivation of efficient nanotextured black silicon solar cells using thermal atomic layer deposition, ACS Appl. Mater. Interfaces 5 (2013) 9752–9759.
[18] C.C. Striemer, P.M. Fauchet, Dynamic etching of silicon for broadband antireflection applications, Appl. Phys. Lett. 81 (2002) 2980–2982.
[19] J.A. Dobrowolski, D. Poitras, P. Ma, H. Vakil, M. Acree, Toward perfect antireflection coatings: numerical investigation, Appl. Opt. 41 (2002) 3075–3083.
[20] E. Garnett, P.D. Yang, Light trapping in silicon nanowire solar cells, Nano Lett. 10 (2010) 1082–1087.
[21] J. Li, H. Yu, S.M. Wong, G. Zhang, X. Sun, P.G.Q. Lo, D.L. Kwong, Si nanopillar array optimization on Si thin films for solar energy harvesting, Appl. Phys. Lett. 95 (2009) 033102.
[22] J. Zhu, C. Hsu, Z. Yu, S. Fan, Y. Cui, Nanodome solar cells with efficient light management and self-cleaning, Nano Lett. 10 (2009) 1979–1984.
[23] G. Conibeer, M. Green, R. Corkish, Y. Cho, E.C. Cho, C.W. Jiang, T. Fangsuwannarak, E. Pink, Y. Huang, T. Puzzer, T. Trupke, B. Richards, A. Shalav, K. Lin, Silicon nanostructures for third generation photovoltaic solar cells, Thin Solid Films 511–512 (2006) 654–662.
[24] W. Wang, S. Wu, K. Reinhardt, Y. Lu, S. Chen, Broadband light absorption enhancement in thin-film silicon solar cells, Nano Lett. 10 (2010) 2012–2018.
[25] E.R.G. Eckert, R.J. Goldstein, E. Pfender, W.E. Ibele, S.V. Patankar, T.W. Simon, N.A. Decker, H. Lee, S.L. Girshick, C.J. Scott, P.J. Strykowski, K.K. Tamma, Heat transfer. A review of 1988 literature, Int. J. Heat Mass Transfer 32 (1989) 2211–2280.
[26] B. Sunden, Transient conduction in a cylindrical shell with a time-varying incident surface heat flux and convective and radiative surface cooling, Int. J. Heat Mass Transfer 32 (1989) 575–584.
[27] Z. Huang, N. Geyer, P. Werner, J. de Boor, U. Gösele, Metal-assisted chemical etching of silicon: a review, Adv. Mater. 23 (2011) 285–308.
[28] B.S. Kim, S. Shin, S.J. Shin, K.M. Kim, H.H. Cho, Control of superhydrophilicity/superhydrophobicity using silicon nanowires via electroless etching method and fluorine carbon coatings, Langmuir 27 (2011) 10148–10156.
[29] B.S. Kim, S. Shin, D. Lee, G. Choi, H. Lee, K.M. Kim, H.H. Cho, Stable and uniform heat dissipation by nucleate-catalytic nanowires for boiling heat transfer, Int. J. Heat Mass Transfer 70 (2014) 23–32.
[30] K.Q. Peng, Y. Wu, H. Fang, X.Y. Zhong, Y. Xu, J. Zhu, Uniform, axial-orientation alignment of one-dimensional single-crystal silicon nanostructure arrays, Angew. Chem. Int. Ed. 44 (2005) 2737–2742.
[31] I. Oh, J. Kye, S. Hwang, Enhanced photoelectrochemical hydrogen production from silicon nanowire array photocathode, Nano Lett. 12 (2011) 298–302.
[32] R. Dewan, M. Marinkovic, R. Noriega, S. Phadke, A. Salleo, D. Knipp, Light trapping in thin-film silicon solar cells with submicron surface texture, Opt. Express 17 (2009) 23058–23065.
[33] K.L. Kelly, E. Coronado, L.L. Zhao, G.C. Schatz, The optical properties of metal nanoparticles: the influence of size, shape, and dielectric environment, J. Phys. Chem. B 107 (2003) 668–677.
[34] X. Zheng, W. Xu, C. Corredor, S. Xu, J. An, B. Zhao, J.R. Lombardi, Laser-induced growth of monodisperse silver nanoparticles with tunable surface plasmon resonance properties and a wavelength self-limiting effect, J. Phys. Chem. C 111 (2007) 14962–14967.
[35] H.A. Atwater, A. Polman, Plasmonics for improved photovoltaic devices, Nat. Mater. 9 (2010) 205–213.
[36] L.M. Liz-Marzán, Tailoring surface plasmons through the morphology and assembly of metal nanoparticles, Langmuir 22 (2006) 32–41.
[37] E. Thouti, N. Chander, V. Dutta, V.K. Komarala, Optical properties of Ag nanoparticle layers deposited on silicon substrates, J. Opt. 15 (2013) 035005.
[38] A. Banerjee, S. Guha, Study of back reflectors for amorphous silicon alloy solar cell application, J. Appl. Phys. 69 (1991) 1030–1035.
[39] K. Yamamoto, M. Yoshimi, Y. Tawada, Y. Okamoto, A. Nakajima, S. Igari, Thin-film poly-Si solar cells on glass substrate fabricated at low temperature, Appl. Phys. A 69 (1999) 179–185.
[40] B.P. Rand, P. Peumans, S.R. Forrest, Long-range absorption enhancement in organic tandem thin-film solar cells containing silver nanoclusters, J. Appl. Phys. 96 (2004) 7519–7526.
[41] T.L. Temple, G.D.K. Mahanama, H.S. Reehal, D.M. Bagnall, Influence of localized surface plasmon excitation in silver nanoparticles on the performance of silicon solar cells, Sol. Energy Mater. Sol. Cells 93 (2009) 1978–1985.
[42] M.D. Kelzenberg, S.W. Boettcher, J.A. Petykiewicz, D.B. Turner-Evans, M.C. Putnam, E.L. Warren, J.M. Spurgeon, R.M. Briggs, N.S. Lewis, H.A. Atwater, Enhanced absorption and carrier collection in Si wire arrays for photovoltaic applications, Nat. Mater. 9 (2010) 239–244.